

## Research Article

# On the Singular Spectrum of the Radiation Operator for Multiple and Extended Observation Domains

**Raffaele Solimene, Maria Antonia Maisto, Giuseppe Romeo, and Rocco Pierri**

*Dipartimento di Ingegneria Industriale e dell'Informazione, Seconda Universita' di Napoli, Via Roma 29, 81031 Aversa, Italy*

Correspondence should be addressed to Raffaele Solimene; [raffaele.solimene@unina2.it](mailto:raffaele.solimene@unina2.it)

Received 26 April 2013; Accepted 26 June 2013

Academic Editor: Francesco Soldovieri

Copyright © 2013 Raffaele Solimene et al. This is an open access article distributed under the Creative Commons Attribution License, which permits unrestricted use, distribution, and reproduction in any medium, provided the original work is properly cited.

The problem of studying how spatial diversity impacts on the spectrum (singular values) of the radiation operator is addressed. This topic is of great importance because of its connection with the so-called number of degrees of freedom concept which in turn is a key parameter in inverse source problems as well as to the problem of transmitting information by waves from a source domain to an observation domain. The case of a bounded rectilinear source with the radiated field observed over multiple bounded rectilinear domains parallel to the source is considered. Then, the analysis is generalized to two-dimensional extended observation domains. Analytical arguments are developed to estimate the pertinent singular value behavior. This allows highlighting the way observation domain features affect spectrum behavior. Numerical examples are shown to support the analytical results.

## 1. Introduction

Determining the number of degrees of freedom (NDF) of the radiated field is one of the classical and most relevant problems in electromagnetics and in optics. This is because the NDF is a crucial parameter which characterizes both forward and inverse source problems. The reader can refer to the paper by Piestun and Miller [1] for a thorough account about how the research on this field has progressed since the pioneering works of Gabor [2] and di Francia [3].

The NDF represents the number of significant and independent parameters needed to represent the radiated field with a given degree of accuracy [4]. Moreover, it is also relevant in inverse source [5] and inverse scattering problems [6] as it is linked to the resolution achievable in the inversions. By interpreting the radiation phenomenon as a way to propagate information from a source domain to an observation domain, the NDF is connected to the question of estimating the number of the available communication channels [7]. This point of view is of fundamental importance in space-time wireless systems and in particular to multiple-input multiple-output (MIMO) communication systems. The link between the electromagnetic NDF and Shannon's information theory has been recently discussed in [8]. The NDF

is also linked to the concepts of the  $\epsilon$ -entropy and  $\epsilon$ -capacity which characterize the topological information theory introduced by Kolmogorov and Tihomirov [9]. In this context, as shown in [10], the NDF gives a measure of the number of  $\epsilon$ -distinguishable messages that can be conveyed back from the noisy data (with  $\epsilon$  being the noise level) in order to recover the source. In that paper, the connection between the topological information theory and Shannon's one has been also discussed [11].

The NDF can be estimated by adopting diffraction arguments or sampling approach [7]. Alternatively, as the radiation operator is a linear nonsymmetric compact operator [12], its singular value decomposition (SVD) [13] provides a further way of tackling the problem. In particular, the singular value decomposition (SVD) should be preferred as it allows for an easier understanding of the flow of information [7]. Moreover, subsets of the range of the radiation operator which are spanned by the singular functions exhibit extremal properties [14]. In other words, exploiting functions which are different from the singular functions leads to the use of more parameters [1].

It is known that the singular values of a compact operator cluster to zero as their index grows. In addition, as the regularity of the kernel increases, the singular values decrease

more and more quickly [15]. Accordingly, since the kernel function of the radiation operator behaves like an entire function of exponential type [16] (when the source and the observation domains do not overlap), the singular values exhibit an abrupt exponential decay beyond a critical index which in general depends on the size of the scatterers, the working frequency, and the observation domain. This has been shown explicitly for some particular configurations for which multipole expansion coincides with the radiation operator spectrum [8, 17]. In these cases, the singular values exhibit an almost step-like behavior [18] (i.e., the radiation operator is almost rank deficient) and the NDF can be quite naturally estimated as the number of singular values preceding the knee. What is more, for such a case Shannon's number (i.e., the operator trace) allows obtaining an NDF estimation without the need of explicitly working out the singular value behavior [19].

In most general cases (as the ones addressed herein), the step-like behavior is not met. In these cases, defying the NDF is not so trivial. Indeed, noise and available a priori information enter the picture so that the NDF becomes dependent on them.

As to the inversion problem, noise and a priori information can be exploited in the regularization procedure. The simplest way to achieve regularization is by numerical filtering, that is, by truncating the SVD expansion in order to establish a compromise between the truncation error and the noise contribution. If the noise level  $\epsilon$  is known and it is assumed that the solution norm is constrained to be  $\leq E$ , then the projections corresponding to the singular values below to  $\epsilon/E$  are discarded [13]. The very popular Tikhonov variational method provides a smoother filtering of the singular values that does not require truncation. However, in practice the reconstruction series must be truncated and the truncation index is usually chosen as above. Note that the same results are achieved if the noise and the unknown source are considered as uncorrelated white Gaussian random process with variance equal to  $\epsilon^2$  and  $E^2$ , respectively [20]. The same results are also obtained by employing the probabilistic approach presented in [21].

Turning to consider the problem from the information point of view, under the same constraints as above, it has been shown that the number of distinguishable messages which can be sent back from data to recover the unknown source is just dependent on the singular values above the threshold  $\epsilon/E$  [10]. Moreover, looking at each one-to-one relationship between the left and the right singular functions as communication channels with gains given by the corresponding singular values, the above condition guaranties that the channels with gain lower than  $\epsilon/E$  convey an amount of Shannon's information which is less than  $\ln 2/2$  [22].

All the previous arguments suggest to identify the NDF by a truncation criterion. Moreover, they highlight the role played by the singular value behavior. Therefore, in this paper we focus on the estimation of the singular value behavior and how spatial diversity effects it. However, it must be remarked that previous constraints, being in some sense global, do not assure that the bulk of the unknown source is recovered nor that the conveyed information is maximized.

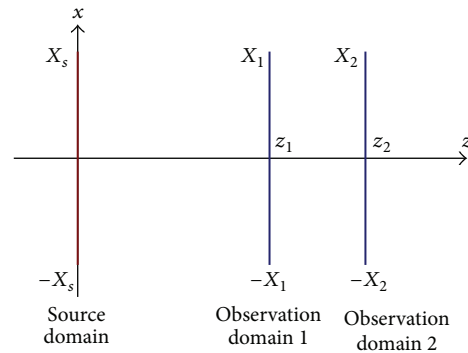


FIGURE 1: Geometry of the problem for the case of two observation domains.

This happens when the source projects significantly over high order singular functions, when the noise is colored, or when some kind of constraints is exploited [8]. In these cases identifying the NDF is more involved and the knowledge of the singular value behavior, even though still important, provides only a partial picture of the problem.

As said above, the focus here is on the estimation of the singular values of the radiation operator when the radiated field is collected over multiple observation domains. For the sake of simplicity, the problem is addressed for a two-dimensional scalar geometry. The source is assumed to be supported over a bounded rectilinear domain, whereas the radiated field is observed either over multiple bounded rectilinear domains or over a two-dimensional observation domain. Green's function is written under the Fresnel zone approximation.

This problem has been addressed previously in [23] for the case of two observation domains. There, by numerical results, it is shown that the second observation domain can lead to a two-step behavior for the singular values. However, the number of significant singular values remains the same as for the single observation case and predictable through a geometrical criterion. Afterwards, the research progressed in [24] where the mathematical rationale of the problem was derived. These results provided a tool to accurately estimate the singular value behavior and to foresee whether a two-step occurs. However, the analysis in [24] was limited to the case of observation domain of the same size. In this contribution we complete the analysis, by extending the results in [24]. To this end, we first consider the complementary situation of two observation domains having different extents but subtending the same observation angular sector. Furthermore, the case of two-dimensional observation domain is addressed.

## 2. Problem Formulation and Mathematical Preliminaries

Let us consider the two-dimensional scalar configuration depicted in Figure 1 where invariance is assumed along the  $y$ -axis.

The field radiated by an electric current  $J$  supported over the segment  $S = [-X_s, X_s]$  of the  $x$ -axis is observed over the observation domain  $O$  located in the Fresnel zone.

Two cases are considered. In the first one, the observation domain consists of an ensemble of segments along the  $x$ -axis at different distances from the source, that is,  $O = \bigcup_m O_m$  with  $O_m = [-X_m, X_m]$  located at  $z_m$ . In the second one, the observation domain  $O \subseteq [-X_{\max}, X_{\max}] \times [z_{\min}, z_{\max}]$ .

In terms of operator notation, in the case of  $M$  observation domains, the radiation phenomenon can be written as

$$\begin{aligned} \mathcal{A} : J \in L^2(S) &\longrightarrow \mathbf{E} \\ &= \{E_1, E_2, \dots, E_M\} \in L^2(O_1) \times L^2(O_2) \cdots \times L^2(O_M), \end{aligned} \quad (1)$$

where, a part from a scalar factor,

$$\begin{aligned} E_m(x_o) &= \frac{\exp(-j\beta z_m)}{\sqrt{z_m}} \\ &\times \int_{-X_s}^{X_s} \exp\left[-j\frac{\beta}{2z_m}(x_o - x)^2\right] J(x) dx \end{aligned} \quad (2)$$

with  $\beta$  being the free-space wavenumber and  $x_o \in [-X_m, X_m]$ .

Instead, for the extended observation domain (1) modifies as

$$\mathcal{A} : J \in L^2(S) \longrightarrow E \in L^2(O), \quad (3)$$

where the operator  $\mathcal{A}$  now reads as

$$\begin{aligned} E(x_o, z_o) &= \frac{\exp(-j\beta z_o)}{\sqrt{z_o}} \\ &\times \int_{-X_s}^{X_s} \exp\left[-j\frac{\beta}{2z_o}(x_o - x)^2\right] J(x) dx. \end{aligned} \quad (4)$$

In (1) and (3),  $L^2(\cdot)$  means the set of square integrable functions supported over the domain enclosed on the brackets. Such functional spaces are equipped with the usual scalar products. More in detail, in the case of multiple domains, it results that

$$\langle \mathbf{f}, \mathbf{g} \rangle_O = \sum_{m=1}^M \int_{-X_m}^{X_m} f_m(x) g_m^*(x) dx, \quad (5)$$

whereas for extended observation domain

$$\langle f, g \rangle_O = \int_{-X_{\max}}^{X_{\max}} \int_{z_{\min}}^{z_{\max}} f(x, z) g^*(x, z) dx dz. \quad (6)$$

In order to estimate the behavior of singular value associated with the operator  $\mathcal{A}$ , in the next sections we tackle the associated eigenvalue problem

$$\mathcal{A}^\dagger \mathcal{A} u_n = \gamma_n u_n, \quad (7)$$

where  $\mathcal{A}^\dagger$  is the adjoint of the operator  $\mathcal{A}$  and  $\gamma_n$ s are the squares of the singular values of the operator  $\mathcal{A}$ . However,

before proceeding further along this path, first some basic mathematical facts are here recalled.

Let us denote by  $\mathcal{B}_\Omega$  the band limiting projector, that is,

$$\mathcal{B}_\Omega f(x) = \frac{1}{2\pi} \int_\Omega F(u) \exp(jux) du \quad (8)$$

so that the  $\mathcal{B}_\Omega f(x)$  spectrum is null for  $u \notin \Omega$ . Here  $\Omega$  is assumed to be a single compact interval but needs not to be centered around the zero frequency.

The spatial limiting projector  $\mathcal{P}_I f(x)$  is defined as

$$\mathcal{P}_I f(x) = \begin{cases} f(x), & x \in I \\ 0, & x \notin I. \end{cases} \quad (9)$$

Furthermore, we introduce the operator  $\mathcal{P}_I \mathcal{B}_\Omega \mathcal{P}_I f(x)$ . When both  $\Omega$  and  $I$  are centered around the zero, this operator assumes the very familiar expression

$$\mathcal{P}_I \mathcal{B}_\Omega \mathcal{P}_I f(x) = \int_{-m(I)/2}^{m(I)/2} \frac{\sin[m(\Omega)/2(x-y)]}{\pi(x-y)} f(y) dy, \quad (10)$$

where  $m(I)$  and  $m(\Omega)$  are the measures of such intervals. This operator has been extensively studied in the literature [25, 26]. It is a compact self-adjoint definite positive operator whose eigenspectrum is given in terms of the prolate spheroidal wave-functions  $u_n(x) = \phi_n(c, x) / \sqrt{\lambda_n(c)}$ . Here,  $c = m(I)m(\Omega)/4$  is the so-called spatial-bandwidth product,  $\phi_n(c, x)$  is the  $n$ th prolate function, and  $\lambda_n(c)$  are the corresponding eigenvalues that enjoy a step-like behavior: they are almost equal to one till the index reaches  $n = [2c/\pi]$ ,  $[\cdot]$  being the greater integer lower than its argument. Beyond such an index they decrease abruptly (i.e., exponentially) to zero.

Having fixed  $m(I)$  and  $m(\Omega)$ , when  $\Omega$  and/or  $I$  are not centered intervals,  $\mathcal{P}_I \mathcal{B}_\Omega \mathcal{P}_I$  is unitary equivalent to the operator (10). Accordingly, eigenvalues hold the same, whereas eigenfunctions are easily linked to  $\phi_n(c, x)$  by unitary transformations.

The following operator plays a crucial role for our analysis:

$$\mathcal{S} = \alpha_1 \mathcal{P}_I \mathcal{B}_{\Omega_1} \mathcal{P}_I + \alpha_2 \mathcal{P}_I \mathcal{B}_{\Omega_2} \mathcal{P}_I, \quad (11)$$

where  $\Omega_1$  and  $\Omega_2$  are disjoint bands and  $\alpha_1$  and  $\alpha_2$  are amplitude factors. As shown in [24], the eigenvalues can be very well approximated in terms of those associated with each single operator. Indeed, if  $c_1$  and  $c_2$  are both greater than one, then

$$\begin{aligned} \mathcal{P}_I \mathcal{B}_{\Omega_1} \mathcal{P}_I u_{n2} &\cong 0, \\ \mathcal{P}_I \mathcal{B}_{\Omega_2} \mathcal{P}_I u_{n1} &\cong 0, \end{aligned} \quad (12)$$

where  $u_{n1}$  and  $u_{n2}$  are the eigenfunctions of  $\mathcal{P}_I \mathcal{B}_{\Omega_1} \mathcal{P}_I$  and  $\mathcal{P}_I \mathcal{B}_{\Omega_2} \mathcal{P}_I$ , respectively. Of course, equality to zero never holds as such operators are positive definite and hence have empty null spaces. In particular, (12) specially holds for either

$n < [2c_1/\pi]$  ( $n < [2c_2/\pi]$ ) or  $n \gg [2c_1/\pi]$  ( $n \gg [2c_2/\pi]$ ). Accordingly, the eigensystem of (11) can be approximated as

$$\begin{aligned} \{u_n[\mathcal{S}]\} &= \{u_{n1}\} \cup \{u_{n2}\}, \\ \{\gamma_n[\mathcal{S}]\} &= \{\alpha_1\lambda_{n1}\} \cup \{\alpha_2\lambda_{n2}\} \end{aligned} \quad (13)$$

that is, as the union of the eigenspectra associated with the two single operators. (From now on, in order to avoid confusion, when necessary, the eigensystem corresponding to an operator  $\mathcal{A}$  will be denoted as  $u_n[\mathcal{A}]$  and  $\gamma_n[\mathcal{A}]$ . The same type of notation will be used also for the singular value decomposition. Instead, we maintain the notation  $\lambda_n$  for the eigenvalues associated with the prolate spheroidal functions, with a clear indication of the spatial-bandwidth product  $\lambda_n(c)$  when necessary.) Hence,  $\gamma_n$  ordered in nonincreasing way exhibit a two-step behavior. The first knee occurs at  $[2c_1/\pi]$  (when  $\alpha_1 > \alpha_2$ ) or  $[2c_2/\pi]$  (for  $\alpha_2 > \alpha_1$ ), whereas the second one is at  $[2c_1/\pi] + [2c_2/\pi]$ . Moreover, the first eigenvalue jump is related to the ratio  $\alpha_1/\alpha_2$ .

We conclude this section by reporting the following proposition which will be useful for the case of extended observation domain.

Let us consider a convolution operator

$$\mathcal{K} : f(x) \in L_I^2 \longrightarrow \mathcal{K}f(x) \in L_I^2 \quad (14)$$

with the kernel function  $k(x) \in L_{\mathfrak{R}}^2$ . Of course, this is a Hilbert-Schmidt operator and it is thus compact. Let us denote with  $K(u)$  the Fourier transform of  $k(x)$ .  $K(u)$  is assumed to be a real positive function and of compact support (i.e.,  $k(x)$  is a bandlimited function)  $\Omega = [u_{\min}, u_{\max}]$ .

Divide now the bandwidth  $\Omega$  in  $M$  subband  $\Omega_m$  each of width  $\Delta = (u_{\max} - u_{\min})/M$  such that  $\Omega_m \cap \Omega_n = \emptyset$  for  $m \neq n$  and  $\Omega = \bigcup_m \Omega_m$ . Further, consider the two sequences

$$\begin{aligned} \bar{K}_1, \bar{K}_2, \dots, \bar{K}_m, \dots, \bar{K}_M, \\ \widehat{K}_1, \widehat{K}_2, \dots, \widehat{K}_m, \dots, \widehat{K}_M, \end{aligned} \quad (15)$$

where

$$\begin{aligned} \bar{K}_m &= \max_{\Omega_m} \{K(u)\}, \\ \widehat{K}_m &= \min_{\Omega_m} \{K(u)\}. \end{aligned} \quad (16)$$

Let us introduce two ‘‘auxiliary’’ operators written as

$$\begin{aligned} \widetilde{\mathcal{K}}f(x) &= \sum_{m=1}^m \bar{K}_m \mathcal{P}_I \mathcal{B}_{\Omega_m} \mathcal{P}_I f(x), \\ \widehat{\mathcal{K}}f(x) &= \sum_{m=1}^M \widehat{K}_m \mathcal{P}_I \mathcal{B}_{\Omega_m} \mathcal{P}_I f(x). \end{aligned} \quad (17)$$

Now, the following proposition can be stated.

Say  $\gamma_n[\widetilde{\mathcal{K}}]$ ,  $\gamma_n[\widehat{\mathcal{K}}]$ , and  $\gamma_n[\mathcal{K}]$ , are the eigenvalues of  $\widetilde{\mathcal{K}}$ ,  $\widehat{\mathcal{K}}$ , and  $\mathcal{K}$ , respectively. Then

$$\gamma_n[\widehat{\mathcal{K}}] \leq \gamma_n(\mathcal{K}) \leq \gamma_n[\widetilde{\mathcal{K}}] \quad \forall n. \quad (18)$$

The proof is omitted but follows from Lemma 3.1 reported in [27].

### 3. Previous Results

We start by recalling previous results concerning the case of two observations domain of equal size  $[-X_1, X_1]$  located at  $z_1$  and  $z_2$ , respectively, with  $z_2 > z_1$ .

In this case, the relevant eigenvalues problem (7) writes explicitly as

$$\begin{aligned} \gamma_n u_n(x) &= \lambda \int_{-X_s}^{X_s} \frac{\sin[\beta(X_1/z_1)(x-x')]}{\pi(x-x')} \\ &\times \exp\left[j\frac{\beta}{2z_1}(x^2-x'^2)\right] u_n(x') dx' \\ &+ \lambda \int_{-X_s}^{X_s} \frac{\sin[\beta(X_2/z_2)(x-x')]}{\pi(x-x')} \\ &\times \exp\left[j\frac{\beta}{2z_2}(x^2-x'^2)\right] u_n(x') dx'. \end{aligned} \quad (19)$$

The eigensystem of operator in (19) is not known in closed form. However, a simple approximated model can be worked out. To this end, it is noted that in Fresnel zone  $1/z$  is a slowly varying function. Therefore, by assuming that  $1/z_1 \approx 1/z_2$  in the exponential terms, (19) can be recast as

$$\gamma_n \tilde{u}_n = 2\lambda P_S B_{\Omega_1} P_S \tilde{u}_n + \lambda P_S B_{\Omega_2} P_S \tilde{u}_n + \lambda P_S B_{\Omega_3} P_S \tilde{u}_n, \quad (20)$$

where  $\Omega_1 = [-\beta X_2/z_2, \beta X_2/z_2]$ ,  $\Omega_2 = [\beta X_2/z_2, \beta X_1/z_1]$ ,  $\Omega_3 = [-\beta X_1/z_1, -\beta X_2/z_2]$  and  $\exp(j\beta/(2z_1)x^2)u_n(x) = \tilde{u}_n(x)$ .

Now, according to results pertinent to operator (11), it results that the eigensystem of (19) can be well approximated by the union of the eigensystem of the three Slepian operators. Hence, the eigenvalues exhibit a two-step behavior:

- (i)  $[2c_1/\pi]$  eigenvalues equal to  $2\lambda$ , due to operator  $\lambda P_S B_{\Omega_1} P_S$ , that determine a step at the index  $N_1 = [2c_1/\pi]$ ,
- (ii)  $[2c_2/\pi] + [2c_3/\pi]$  eigenvalues equal to  $\lambda$ , due to  $\lambda P_S B_{\Omega_2} P_S$  and  $\lambda P_S B_{\Omega_3} P_S$  operators, that determine a step at the index  $N_2 = N_1 + [2c_2/\pi] + [2c_3/\pi]$ ,
- (iii) other eigenvalues almost 0 due to eigenvalues of the three operators that decay exponentially.

In particular, the above theory allows to forecast a single step behavior when the integer parts of the last two addends in the expression of  $N_2$  are zeros. In general, we expect a double-step behavior for the singular values.

More details and the numerical check of this result are reported in [24]. In particular, previous model holds true even  $z_2 \gg z_1$ .

Hence, for the two-observation domains of equal size it can be concluded that the second domain entails a two-step behavior for the singular values. Therefore, the NDF depends on the noise that set the threshold above which the singular values can be considered significant. If significant means as compared with zero then the NDF coincides with that obtainable by using the single observation domain which subtends the largest observation angular sector, that

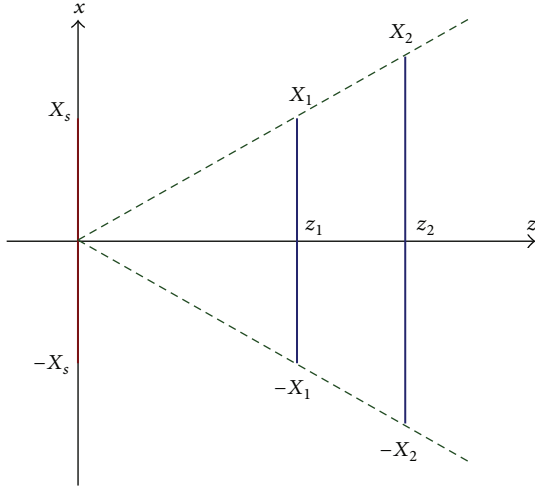


FIGURE 2: Geometry of the problem for the case of two observation domains which subtend the same observation angular sector.

is,  $\max\{X_1/z_1, X_2/z_2\}$ . However, as part of the singular values have higher amplitude, the strength of the connection is increased [7]. Equivalently, while tackling the inverse problem, the inversion is expected to be more stable.

As a concluding remark we note that previous analysis can be easily adapted to account for more than two observation domains. In this case singular values will exhibit a multistep behavior as long as the spatial-bandwidth products involved in the pertinent version of (20) are all sufficiently greater than one.

#### 4. Two Observation Domains That Subtend the Same Angular Sector

We now turn to address the case when the two observation domains subtend the same observation angular sector (see Figure 2). This means that we assume  $X_1/z_1 = X_2/z_2$ .

Under the same assumption as in previous section (20) particularizes as

$$\gamma_n \tilde{u}_n = 2\lambda P_S B_\Omega P_S \tilde{u}_n \quad (21)$$

with  $\Omega = [-\beta X_2/z_2, \beta X_2/z_2]$  (or equivalently  $\Omega = [-\beta X_1/z_1, \beta X_1/z_1]$ ). This is now a standard Slepian operator whose eigenvalues have a step-like behavior with the knee occurring at  $N = \lceil 2c/\pi \rceil$ , with  $c = \beta X_2 X_s / z_2$ . Therefore, it can be readily concluded that by adding further observation domains which subtend the same observation sector does not change the single step behavior which pertains the single observation domain. Rather, this leads to only an increase of the numerical value of the singular values across their flat part.

This result as well as the one recalled in the previous section can have a simple interpretation from the diffraction arguments perspective. Indeed, the eigenvalue two-step behavior could be expected if the observation domains are characterized in terms of the angular sectors they subtend. In fact, the first stronger flat region can be seen as being

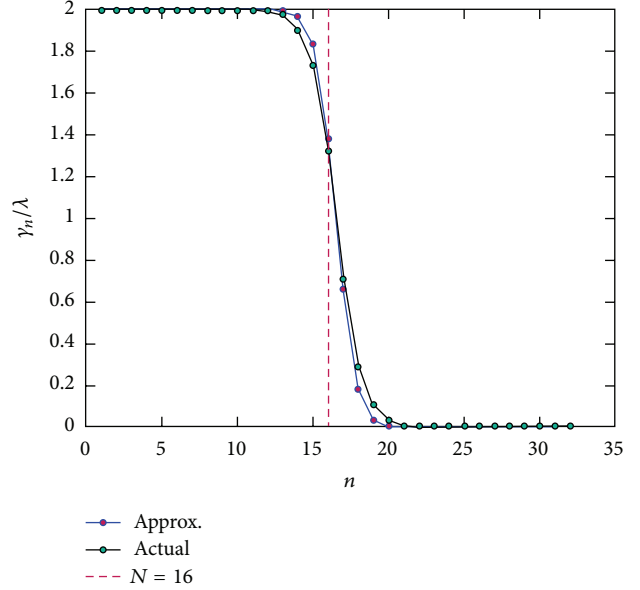


FIGURE 3: Two observation domains that subtend the same angular sector for the case of  $X_s = 20\lambda$ ,  $X_1 = 20\lambda$ ,  $X_2 = 25\lambda$ ,  $z_1 = 100\lambda$ , and  $z_2 = 125\lambda$ . Comparison between the squared singular values of the radiation operator (denoted as actual) and the eigenvalues of the approximate model given by (21) (denoted as approx.).

due to the information collected over  $O_1$  and  $O_2$  under the angular sector subtended by  $O_2$  (which is common to both observation domains) and the second flat region as being due to only  $O_1$  and collected under the remaining directions belonging to the angular sector subtended by  $O_1$ . Therefore, when  $O_1$  and  $O_2$  subtend the same angular sector, a single flat part must be observed with the numeric value of the singular values doubled with respect to the single observation case.

These arguments are convincing and very well verified in Figure 3.

However, when the distance between the two observation domains is increased, the singular values of the radiation operator no longer enjoy the single step behavior. Indeed, as shown in Figure 4, despite the fact that the theory developed so far would predict the same behavior as in Figure 3, now the singular values exhibit a two-step behavior. More interestingly, the knee of the second step occurs at an index greater than the one that would be expected according to the observation angular sector.

It is clear that this means that the approximated model employed to derive (21) does not work any longer. Hence, it is necessary to take a step back in order to better analyze the model. To this end, we relax the hypothesis that  $1/z_1 \approx 1/z_2$  and rewrite (19) as

$$\begin{aligned} \gamma_n \hat{u}_n(x) &= \lambda \int_{-X_s}^{X_s} \frac{\sin[\beta(X_1/z_1)(x-x')] }{\pi(x-x')} \\ &\times \exp\left[j\frac{\beta\Delta}{2}(x^2-x'^2)\right] \hat{u}_n(x') dx' \end{aligned}$$

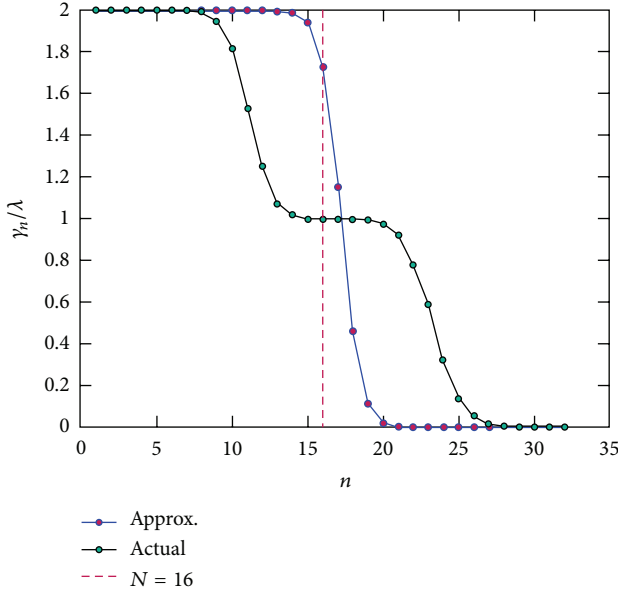


FIGURE 4: Two observation domains that subtend the same angular sector for the case of  $X_s = 50\lambda$ ,  $X_1 = 20\lambda$ ,  $X_2 = 50\lambda$ ,  $z_1 = 240\lambda$ , and  $z_2 = 600\lambda$ . Comparison between the squared singular values of the radiation operator (denoted as actual) and the eigenvalues of the approximate model given by (21) (denoted as approx.).

$$\begin{aligned}
 & + \lambda \int_{-X_s}^{X_s} \frac{\sin[\beta(X_2/z_2)(x-x')]}{\pi(x-x')} \\
 & \times \exp\left[-j\frac{\beta\Delta}{2}(x^2-x'^2)\right] u_n(x') dx'
 \end{aligned} \quad (22)$$

with  $\Delta = (1/z_1 - 1/z_2)/2$ ,  $1/z = (1/z_1 + 1/z_2)/2$  and  $\hat{u}_n(x) = \exp[-j\beta x^2/(2z)]\hat{u}_n(x)$ .

Now we can do the following approximation for the exponentials appearing in (22)

$$\begin{aligned}
 \exp\left[\pm\frac{j\beta\Delta(x^2-x'^2)}{2}\right] & = \exp\left[\pm\frac{j\beta\Delta(x+x')(x-x')}{2}\right] \\
 & \approx \exp\left[\pm\frac{j\beta\Delta X_s(x-x')}{2}\right].
 \end{aligned} \quad (23)$$

This approximation can be justified by observing that the exponential factor can be interpreted as a modulating term for the kernel function. Therefore, posing  $x+x' = X_s$  is equivalent to choosing the intermediate frequency of modulation. Note that this model also includes the approximation previously discussed as a particular case when  $\Delta = 0$  is assumed.

Accordingly, (22) becomes

$$\begin{aligned}
 \gamma_n \hat{u}_n(x) & = \lambda \int_{-X_s}^{X_s} \frac{\sin[\beta(X_1/z_1)(x-x')]}{\pi(x-x')} \\
 & \times \exp\left[j\frac{\beta\Delta}{2}X_s(x-x')\right] \hat{u}_n(x') dx' \\
 & + \lambda \int_{-X_s}^{X_s} \frac{\sin[\beta(X_2/z_2)(x-x')]}{\pi(x-x')} \\
 & \times \exp\left[-j\frac{\beta\Delta}{2}X_s(x-x')\right] \hat{u}_n(x') dx'.
 \end{aligned} \quad (24)$$

Let us define the following ‘‘spatial’’ frequencies  $a = -\beta(\Delta/2)X_s - \beta(X_2/z_2)$ ,  $b = -\beta(\Delta/2)X_s + \beta(X_2/z_2)$ ,  $c = \beta(\Delta/2)X_s - \beta(X_1/z_1)$ , and  $d = \beta(\Delta/2)X_s + \beta(X_1/z_1)$ , and assume that  $b \geq c$ . Then, (24) can be rearranged as

$$\gamma_n \hat{u}_n = \lambda P_S B_{\Omega_3} P_S \hat{u}_n + 2\lambda P_S B_{\Omega_2} P_S \hat{u}_n + \lambda P_S B_{\Omega_1} P_S \hat{u}_n, \quad (25)$$

where  $\Omega_1 = [\min(a, c), \max(a, c)]$ ,  $\Omega_2 = [\max(a, c), b]$  and  $\Omega_3 = [b, d]$ .

At this point, we can apply the same reasoning as done in the previous section and exploit results of (11). By doing so we obtain that

- (i)  $[2c_2/\pi]$  eigenvalues close to  $2\lambda$ , due to operator  $2\lambda P_S B_{\Omega_2} P_S$ , that determines a step at the index  $N_1 = [2c_2/\pi]$ ,
- (ii)  $[2c_1/\pi] + [2c_3/\pi]$  eigenvalues close to  $\lambda$ , due to  $\lambda P_S B_{\Omega_1} P_S$  and  $\lambda P_S B_{\Omega_3} P_S$  operators, that determine a step at the index  $N_2 = N_1 + [2c_1/\pi] + [2c_3/\pi]$ ,
- (iii) eigenvalues close to 0 due to the three operators, beyond  $N_2$ .

By looking at Figure 5, where the example of Figure 4 is rerun, it is seen that now the new approximated model works fairly well in predicting the squared singular values of the radiation operator as the two-step behavior is very well reproduced.

## 5. Extended Observation Domains

Previous results can be trivially generalized to the case of multiple observation domains. However, the same theoretical arguments can be applied as long as the spatial-bandwidth products occurring while arranging the pertinent operator as in (20) or (25) are sufficiently greater than one. In [28], it is shown that each spatial-bandwidth product  $c$  can be as low as 4. This puts a limit on the number of rectilinear observation domains that can be taken within a fixed extent along  $z$  of the observation domain.

This drawback can be completely avoided if the problem is directly cast by considering a two-dimensional observation domain. The cases that will be addressed herein are sketched in Figure 6.

Let us start from the configuration reported in Figure 6(a).

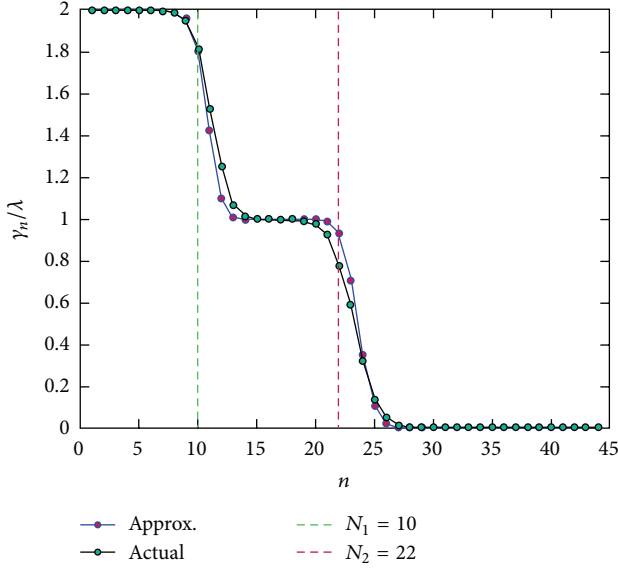


FIGURE 5: Two observation domains that subdivide the same angular sector for the case of  $X_s = 50 \lambda$ ,  $X_1 = 20 \lambda$ ,  $X_2 = 50 \lambda$ ,  $z_1 = 240 \lambda$ , and  $z_2 = 600 \lambda$ . Comparison between the squared singular values of the radiation operator (denoted as actual) and the eigenvalues of the approximate model given by (25) (denoted as approx.).

In this case it results that

$$\begin{aligned} \mathcal{A}^\dagger \mathcal{A} u_n(x) &= \lambda \int_{-X_s}^{X_s} \int_{z_{\min}}^{z_{\max}} \frac{\sin[\beta(X_1/z)(x-x')]}{\pi(x-x')} \\ &\quad \times \exp\left[j\frac{\beta}{2z}(x^2-x'^2)\right] dz u_n(x') dx', \end{aligned} \quad (26)$$

By adopting the same approximation as done for the domains of equal extent, (26) can be rewritten as

$$\begin{aligned} \mathcal{A}^\dagger \mathcal{A} \tilde{u}_n(x) &= \lambda \int_{-X_s}^{X_s} \int_{z_{\min}}^{z_{\max}} \frac{\sin[\beta(X_1/z)(x-x')]}{\pi(x-x')} dz \tilde{u}_n(x') dx'. \end{aligned} \quad (27)$$

with  $\tilde{u}_n(x) = u_n(x) \exp[-j\beta x^2/(2z_{\min})]$ .

Hence, the problem is cast as the study of the convolution operator (27) whose kernel function  $k(x)$  has a Fourier transform given by

$$K(u) = \begin{cases} z_{\max} - z_{\min} & |u| \leq \frac{\beta X_1}{z_{\max}} \\ \left| \frac{\beta X_1}{u} \right| - z_{\min} & \frac{\beta X_1}{z_{\max}} \leq |u| \leq \frac{\beta X_1}{z_{\min}} \\ 0 & \text{elsewhere.} \end{cases} \quad (28)$$

When  $(\beta X_1/z_{\min} - \beta X_1/z_{\max})X_1 \leq 1$ , then

$$\mathcal{A}^\dagger \mathcal{A} \approx (z_{\max} - z_{\min}) \mathcal{P}_S \mathcal{B}_{\Omega_0} \mathcal{P}_S \quad (29)$$

with  $\Omega_0 = [-\beta X_1/z_{\max}, \beta X_1/z_{\max}]$ . Therefore, the eigenvalues of (26) (and hence the singular values of the corresponding radiation operator) are very well approximated by a step-like behavior. This is shown in Figure 7. Hence, the NDF basically remains the same as the single observation domain. On the contrary, the numerical values across the flat part have drastically increased at  $(z_{\max} - z_{\min})$ , which for the presented example is 10.

Approximation in (29) cannot be invoked if the extent of the observation domain along  $z$  is increased. Then, according to the proposition reported at the end of Section 2, we can construct the two auxiliary operators

$$\begin{aligned} \widehat{\mathcal{A}^\dagger \mathcal{A}} &= (z_{\max} - z_{\min}) \mathcal{P}_S \mathcal{B}_{\Omega_0} \mathcal{P}_S \\ &\quad + \sum_{m=1}^M \widetilde{K}_m \left( \mathcal{P}_S \mathcal{B}_{\widetilde{\Omega}_m} \mathcal{P}_S + \mathcal{P}_S \mathcal{B}_{\widetilde{\Omega}_m} \mathcal{P}_S \right), \end{aligned} \quad (30)$$

$$\begin{aligned} \widehat{\mathcal{A}^\dagger \mathcal{A}} &= (z_{\max} - z_{\min}) \mathcal{P}_S \mathcal{B}_{\Omega_0} \mathcal{P}_S \\ &\quad + \sum_{m=1}^M \widehat{K}_m \left( \mathcal{P}_S \mathcal{B}_{\widehat{\Omega}_m} \mathcal{P}_S + \mathcal{P}_S \mathcal{B}_{\widehat{\Omega}_m} \mathcal{P}_S \right), \end{aligned}$$

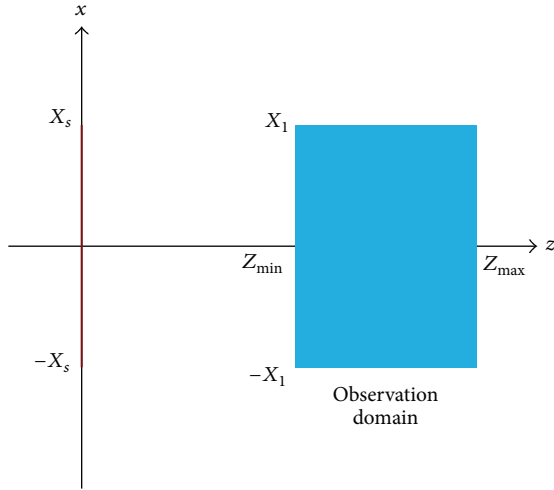
where  $\widetilde{\Omega}_m = [\beta X_1/z_{\max} + (m-1)\Delta, \beta X_1/z_{\max} + m\Delta]$  and  $\widehat{\Omega}_m = [-\beta X_1/z_{\max} - m\Delta, -\beta X_1/z_{\max} - (m-1)\Delta]$ ,  $\Delta = (\beta X_1/z_{\min} - \beta X_1/z_{\max})/M$ ,  $2M$  being the number of bands used to divide the frequency interval  $\beta X_1/z_{\max} \leq |u| \leq \beta X_1/z_{\min}$ . Moreover, the sequences  $\widetilde{K}_m$  and  $\widehat{K}_m$  are chosen as described in Section 2.

Now, as long as  $c_M = X_1 \Delta/2$  is sufficiently greater than 1 (in the sense explained above), the eigenvalues of  $\widehat{\mathcal{A}^\dagger \mathcal{A}}$  and  $\widetilde{\mathcal{A}^\dagger \mathcal{A}}$  can be foreseen by applying the same reasoning as in (11). Accordingly, they can be used to estimate those of  $\mathcal{A}^\dagger \mathcal{A}$ . The way to achieve that is summarized in the following statement.

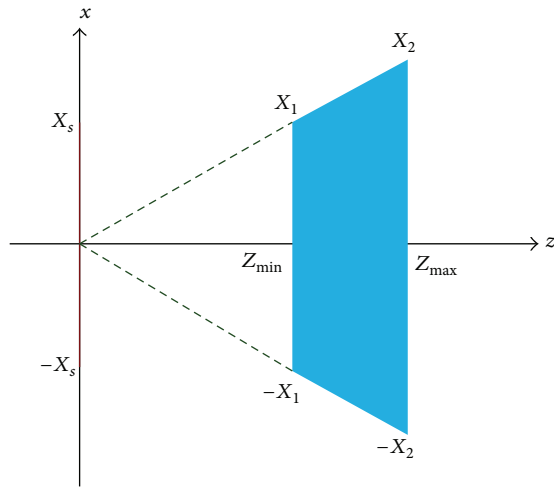
*Statement 1.* Let  $N(\tau_{th}, c) = \#\{\gamma_n[\mathcal{A}^\dagger \mathcal{A}] \geq \tau_{th}\}$  be the number of eigenvalues of  $\mathcal{A}^\dagger \mathcal{A}$  which are greater than  $\tau_{th}$ . Say  $N_0 = \lfloor \beta X_1/z_{\max} X_1 \rfloor$ . If  $c_M \gg 1$ , and hence  $c = \beta X_1/z_{\min} X_1$ , then it approximately holds that

$$\begin{aligned} N(\tau_{th}, c) &\leq N_0 + 2m \left\lceil \frac{2c_M}{\pi} \right\rceil \quad \widetilde{K}_m < \tau_{th}, \\ N(\tau_{th}, c) &\geq N_0 + 2m \left\lceil \frac{2c_M}{\pi} \right\rceil \quad \tau_{th} < \widehat{K}_m, \quad m \neq M, \\ N(\tau_{th}, c) &\approx \left\lceil \frac{2c}{\pi} \right\rceil \quad \widetilde{K}_M > \tau_{th}. \end{aligned} \quad (31)$$

The goodness of this statement can be appreciated by the example reported in Figure 8. As expected, the first  $N_0$  eigenvalues are almost constant. Beyond such an index, however, the eigenvalues decay more gracefully than the previous case. Furthermore, the role of the observation extent along  $z$  is still more evident than in the result of Figure 7.



(a)



(b)

FIGURE 6: Geometries of the problem for the case of two-dimensional observation domain.

Indeed, the numerical value of the eigenvalues are greatly increased (up to  $z_{\max} - z_{\min} = 100$  times) than the single observation domain.

The same analysis can be repeated for the observation domain depicted in Figure 6(b). For such a case we have that

$$\begin{aligned} \mathcal{A}^\dagger \mathcal{A} u_n(x) &= \lambda \int_{-X_s}^{X_s} \frac{\sin[\beta\alpha(x-x')]}{\pi(x-x')} \\ &\times \int_{z_{\min}}^{z_{\max}} \exp\left[j\frac{\beta}{2Z} X_s(x-x')\right] dz u_n(x') dx', \end{aligned} \quad (32)$$

where  $\alpha$  denotes the observation angular sector and the same approximation as in (24) has been exploited.

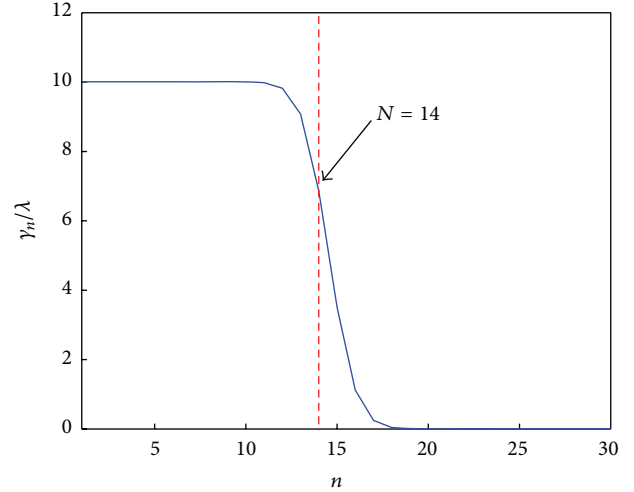


FIGURE 7: Eigenvalue behavior for a rectangular two-dimensional observation domain with  $X_s = 20\lambda$ ,  $X_1 = 20\lambda$ ,  $X_2 = 20\lambda$ ,  $z_1 = 110\lambda$ , and  $z_2 = 120\lambda$ .

Also here, a convolution operator has to be studied but now the kernel function  $k(x)$  has a Fourier transform given by

$$K(u) = \begin{cases} z_{\max} - z_{\min} & \frac{\beta X_s}{2z_{\min}} - \beta\alpha \leq u \leq \frac{\beta X_s}{2z_{\max}} + \beta\alpha \\ \frac{\beta X_s}{2(u - \beta\alpha)} - z_{\min} & \frac{\beta X_s}{2z_{\max}} + \beta\alpha < u < \frac{\beta X_s}{2z_{\min}} + \beta\alpha \\ z_{\max} - \frac{\beta X_s}{2(u + \beta\alpha)} & \frac{\beta X_s}{2z_{\max}} - \beta\alpha < u < \frac{\beta X_s}{2z_{\min}} - \beta\alpha \\ 0 & \text{elsewhere} \end{cases} \quad (33)$$

when  $X_s/2(1/z_{\min} - 1/z_{\max}) < 2\alpha$ .

Finally, a statement similar to Statement 1 can be easily derived which allows to foreseen the singular value behavior.

## 6. Conclusion

In this paper, we continued the research on the way the spatial diversity impacts on the singular value behavior of the radiation operator we started in the papers [23, 24].

As in those papers, here the study has been developed for a canonic two-dimensional scalar configuration where the source and the observation domains were represented by bounded parallel strips. Also the case of an extended observation domain has been addressed. These simple scenarios allowed us to develop analytical arguments which clearly permitted to estimate (also quantitatively) the singular value behavior. In particular, for the case of a two-dimensional observation domain, upper and lower bounds for the singular values have been determined: these permitted to estimate the number of singular values which are above a given threshold. It is important to remark that the method developed for



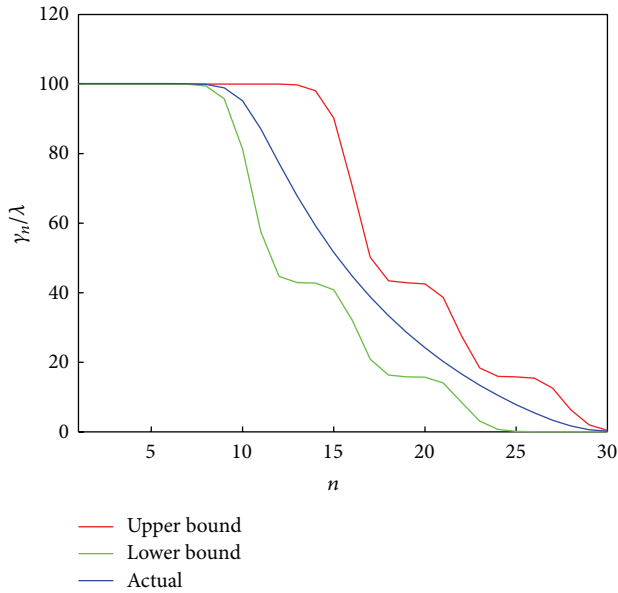


FIGURE 8: Eigenvalue behavior for a rectangular two-dimensional observation domain with  $X_s = 20\lambda$ ,  $X_1 = 20\lambda$ ,  $X_2 = 20\lambda$ ,  $z_1 = 60\lambda$ , and  $z_2 = 160\lambda$ .

addressing two-dimensional observation domains provides a tool for analyzing more general convolution operators provided that they are of Hilbert-Schmidt class.

It has been shown that the main effect of considering multiple observation domains is a shaping and a magnitude amplification of the singular values. In particular, magnitude increasing can be considerable in the case of extended observation domains as it is proportional to its size  $z_{\max} - z_{\min}$  along depth. Moreover, it has been shown that the number of significant singular values can be greater than those predicted by conventional diffraction arguments. In particular, this happens when the observation domains subtend the same angular sector and are sufficiently apart from each other.

The addressed problem and the obtained results are relevant not only from the mathematical point of view but also for classical electromagnetic problems such as the inverse source and the transmission of information. This is because the singular values of the radiation operator are intimately connected to the concept of NDF. Indeed, when some global constraints are employed (as discussed in the introduction), the number of relevant singular values right coincide with the NDF. Under this circumstance, the results described above can be rephrased by saying that spatial diversity can allow for a more stable inversion procedure, or by changing perspective, that it entails a significant growth on the information content [10].

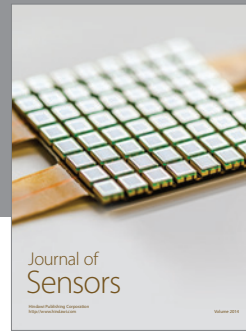
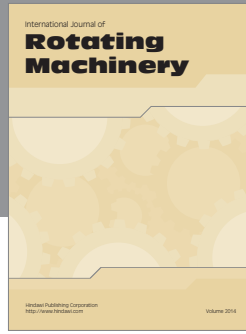
As a concluding remark, we note that the extension of the present research to the case of a planar source and a volumetric observation domain is rather simple as in the Fresnel zone the kernel factorizes with respect to the two transversal coordinates. Furthermore, addressing far zone cases is even more simple. Instead, making the observation

domains in the source near zone appears more complicated. We defer this topic for future developments.

## References

- [1] R. Piestun and D. A. B. Miller, "Electromagnetic degrees of freedom of an optical system," *Journal of the Optical Society of America A*, vol. 17, no. 5, pp. 892–902, 2000.
- [2] D. Gabor, "Light and information," in *Progress in Optics*, E. Wolf, Ed., vol. 1, pp. 111–153, North Holland Elsevier, Amsterdam, The Netherlands, 1990.
- [3] G. T. di Francia, "Degrees of freedom of an image," *Journal of the Optical Society of America*, vol. 59, no. 7, pp. 799–804, 1969.
- [4] O. M. Bucci and G. Franceschetti, "On the degrees of freedom of scattered fields," *IEEE Transactions on Antennas and Propagation*, vol. 37, no. 7, pp. 918–926, 1989.
- [5] R. Pierri, A. Liseno, F. Soldovieri, and R. Solimene, "In-depth resolution for a strip source in the Fresnel zone," *Journal of the Optical Society of America A*, vol. 18, no. 2, pp. 352–359, 2001.
- [6] R. Solimene, G. Leone, and R. Pierri, "Resolution in two-dimensional tomographic reconstructions in the Fresnel zone from Born scattered fields," *Journal of Optics A*, vol. 6, no. 6, pp. 529–536, 2004.
- [7] D. A. Miller, "Communicating with waves between volumes: evaluating orthogonal spatial channels and limits on coupling strengths," *Applied Optics*, vol. 39, no. 11, pp. 1681–1699, 2000.
- [8] F. K. Gruber and E. A. Marengo, "New aspects of electromagnetic information theory for wireless and antenna systems," *IEEE Transactions on Antennas and Propagation*, vol. 56, no. 11, pp. 3470–3484, 2008.
- [9] A. N. Kolmogorov and V. M. Tihomirov, "ε-entropy and ε-capacity of sets in functional spaces," *Transactions of the American Mathematical Society*, vol. 17, pp. 277–364, 1961.
- [10] E. De Micheli and G. A. Viano, "Fredholm integral equation of the first kind and topological information theory," *Integral Equations and Operator Theory*, vol. 73, no. 4, pp. 553–571, 2012.
- [11] E. De Micheli and G. A. Viano, "Metric and probabilistic information associated with Fredholm integral equation of the first kind," *Journal of Integral Equations and Applications*, vol. 14, no. 3, pp. 283–310, 2002.
- [12] F. Riesz and B. Nagy, *Functional Analysis*, Dover, New York, NY, USA, 1990.
- [13] M. Bertero, "Linear inverse and ill-posed problems," *Advances in Electronics and Electron Physics C*, vol. 75, pp. 1–120, 1989.
- [14] D. Jagerman, "ε-entropy and approximation of bandlimited functions," *SIAM Journal on Applied Mathematics*, vol. 17, no. 2, pp. 362–377, 1969.
- [15] E. Hille and J. D. Tamarkin, "On the characteristic values of linear integral equations," *Acta Mathematica*, vol. 57, no. 1, pp. 1–76, 1931.
- [16] A. Requicha, "The zeros of entire functions: theory and engineering applications," *Proceedings of the IEEE*, vol. 68, no. 3, pp. 308–328, 1980.
- [17] A. Brancaccio, G. Leone, and R. Pierri, "Information content of Born scattered fields: results in the circular cylindrical case," *Journal of the Optical Society of America A*, vol. 15, no. 7, pp. 1909–1917, 1998.
- [18] F. Gori, "Integral equations for incoherent anagery," *Journal of the Optical Society of America*, vol. 64, no. 9, pp. 1237–1243, 1974.

- [19] F. Gori and G. Guattari, "Shannon number and degrees of freedom of an image," *Optics Communications*, vol. 7, no. 2, pp. 163–165, 1973.
- [20] M. Bendinelli, A. Consortini, L. Ronchi, and B. R. Frieden, "Degrees of freedom, and eigenfunctions, for the noisy image," *Journal of the Optical Society of America*, vol. 64, no. 11, pp. 1498–1502, 1974.
- [21] E. De Micheli, N. Magnoli, and G. A. Viano, "On the regularization of fredholm integral equations of the first kind," *SIAM Journal on Mathematical Analysis*, vol. 29, no. 4, pp. 855–877, 1998.
- [22] E. De Micheli and G. A. Viano, "Probabilistic regularization in inverse optical imaging," *Journal of the Optical Society of America A*, vol. 17, no. 11, pp. 1942–1951, 2000.
- [23] R. Pierri and F. Soldovieri, "On the information content of the radiated fields in the near zone over bounded domains," *Inverse Problems*, vol. 14, no. 2, pp. 321–337, 1998.
- [24] R. Solimene and R. Pierri, "Number of degrees of freedom of the radiated field over multiple bounded domains," *Optics Letters*, vol. 32, no. 21, pp. 3113–3115, 2007.
- [25] D. Slepian and H. O. Pollak, "Prolate spheroidal wave function, Fourier analysis and uncertainty-I," *Bell System Technical Journal*, vol. 40, pp. 43–63, 1961.
- [26] H. J. Landau and H. O. Pollak, "Prolate spheroidal wave function, Fourier analysis and uncertaintyII," *Bell System Technical Journal*, vol. 40, pp. 64–84, 1961.
- [27] G. Newsam and R. Barakat, "Essential dimension as a well-defined number of degrees of freedom of finiteconvolution operators appearing in optics," *Journal of the Optical Society of America A*, vol. 2, no. 11, pp. 2040–2045, 1985.
- [28] R. Solimene, R. Barresi, and G. Leone, "Localizing a buried planar perfect electric conducting interface by multi-view data," *Journal of Optics A*, vol. 10, no. 1, Article ID 015010, pp. 1–10, 2008.



**Hindawi**

Submit your manuscripts at  
<http://www.hindawi.com>

